*Int. J. Solids Structures* Vol. 16, pp. 313–328

0020-7683/80/0401-0313/$02.00/0

# BUCKLING OF ELASTIC–PLASTIC DISCRETELY STIFFENED CYLINDERS IN AXIAL COMPRESSION

B. D. REDDY†

Departments of Applied Mathematics and Civil Engineering, University of Cape Town, Private Bag, Rondebosch 7700, South Africa

(*Received* 12 *December* 1978; *in revised form* 21 *March* 1979)

**Abstract**—Bifurcation under axial compression of discretely stringer-stiffened cylinders in the elastic and plastic ranges is studied. The stiffeners are treated as long plates. Small-strain $J_2$ flow and deformation theories of plasticity are used. The effect of stiffener size on the critical stress is investigated; this is discussed with reference to the critical stresses of an equivalent simply-supported panel, and of a long plate simply-supported on three edges and free along one longitudinal edge. The effects of stiffener eccentricity, and of the number of stiffeners, is also discussed.

## NOTATION

$A_j$ $(j = 1, \ldots, 4)$ amplitudes of eigenmode, eqn (35)
$A_p$ area of typical panel
$A_s$ cross-sectional area of typical stiffener
$b_{\alpha\beta}$ curvature tensor
$\bar{C}^{ij}_{kl}$ coefficients in three-dimensional constitutive law, eqn (11)
$C^{\alpha\beta\kappa\gamma}$ plane-stress coefficients, eqn (16)
$C_{ij}$ coefficients relating effective stress—rates to mid-surface strain-rates, eqn (19)
$d$ half-depth of stiffener
$D$ variable in constitutive relations, eqns (20) and (21)
$e$ eccentricity of stiffener
$E$ Young's modulus
$E_s$ Secant modulus
$E_t$ tangent modulus
$E_{\alpha\beta}$ strain tensor of stiffeners
$F$ functional to be tested for bifurcation
$g_{ij}$ metric tensor of panels
$h_1$, $h_2$, $h_2' = \mathrm{d}h_2/\mathrm{d}J_2$ coefficients in constitutive relations, eqns (13), (14)
$J_2$ second invariant of stress deviator tensor
$K_{\alpha\beta}$ curvature tensor of stiffeners
$l$ length of shell
$m^{\alpha\beta}$, $M^{\alpha\beta}$ bending moment tensors for panels and stiffeners
$m_{(x,x\theta,\theta)}$, $M_{(x,xy,y)}$ physical components of bending moment tensors
$n^{\alpha\beta}$, $N^{\alpha\beta}$ stress resultant tensors for panels and stiffeners
$n_{(x,x\theta,\theta)}$, $N_{(x,xy,y)}$ physical components of stress resultant tensors
$n$ strain-hardening exponent, eqn (15)
$N$ number of stiffeners
$P$ total load acting on shell
$r$ radius of panels
$S_{(\ldots)}$ dimensionless stress, equal to $\sigma(\ldots)/\sigma_{cu}$ (Table 1)
$S^{ij}$ stress deviator tensor
$t$ thickness of panels
$t_s$ thickness of stiffeners
$u^\alpha$, $U^\alpha$ Components of mid-surface displacements in panels and stiffeners, respectively
$(u, v, w)$, $(U, V, W)$ physical components of displacements in axial, tangential and lateral directions
$x$ axial coordinate
$y$ tangential coordinate in stiffeners
$z, Z$ normal coordinate in panels and stiffeners, respectively

*Greek symbols*

$\alpha$ $= m\pi r/l$, where $m$ = number of longitudinal half-waves
$\bar{\beta}; \beta$ variables in solution to characteristic eqns (33)–(35)
$\epsilon_{\alpha\beta}$ mid-surface strain tensor in panels
$\epsilon_x, \epsilon_\theta, \gamma_{x\theta}$ physical components of $\epsilon_{\alpha\beta}$
$\eta_{ij}$ strain tensor
$\theta$ circumferential coordinate of panel
$\theta_0$ half "width" of panels
$\kappa_{\alpha\beta}$ bending strain tensor of panels

$\mu_{1j}, \mu_{2j}$ variables in eigenmode, eqns (36) and (37)
$\nu$ Poisson's ratio
$\xi$ dimensionless axial coordinate, $\equiv x/r$
$\sigma_c$ critical stress of stiffened shell
$\sigma_{cruc}$ critical stress of cruciform column, eqn (50)
$\sigma_{cu}$ critical stress of *elastic* unstiffened cylinder, eqn (49)
$\sigma_{panel}$ critical stress of simply-supported cylindrical panel having dimensions of panels in stiffened shell
$\sigma_{st}$ critical stress of stiffener treated as long plate, simply supported on three sides and free on one longitudinal edge
$\sigma_x$ prebuckling stress
$\sigma_y$ yield stress in simple tension

*Superscripts*

$(\dot{\ldots})$ denotes the rate of change of $(\ldots)$ w.r.t. any monotonically varying quantity
$(\ldots)^{(i)}$ denotes $(\ldots)$ referred to $i$th panel or stiffener
$(\hat{\ldots})$ denotes difference between increments of $(\ldots)$ on fundamental path and on bifurcated path.

## 1. INTRODUCTION

Most of the research on stringer-stiffened cylinders in axial compression has hitherto been confined to the case in which the stiffeners are closely spaced. Analyses for linear-elastic materials are then carried out by assuming that stiffener properties can be "smeared out", to give an equivalently orthotropic shell. Such analyses have given results which are in reasonable accord with experimental data[1]. Furthermore, the critical mode is an overall mode, in the sense that half-waves in the circumferential direction extend over a number of stiffeners.

When shell is sparsely stiffened, the mode in the circumferential direction is likely to be a local mode between stiffeners. Koiter[2] has considered this problem in the elastic range, and has obtained results for the critical and initial post-critical behaviour on the assumption that the stiffeners have negligible torsional rigidity and that no axial waves form along panel-stiffener junctions. This enabled Koiter to consider only a typical panel between stiffeners. On this basis it was shown that the post-critical behaviour is stable for sufficiently flat panels, while more curved panels have unstable post-critical behaviour.

Stephens[3] has extended Koiter's[2] analysis by examining the critical and post-critical behaviour of an axially compressed cylindrical panel, with the longitudinal edges of the panel partially restrained against bending in the circumferential direction: this restraint was effected by relating the edge bending moment of the panel to the torsional moment in the stringer.

Stephens also included the effects of internal pressure in his analysis, and showed that the effect of torsional rigidity of the stiffeners, as well as that of internal pressure, was to increase the critical load and reduce the sensitivity of the structure to imperfections.

Wang and Lin[4] analysed the bifurcation problem of a discretely-stiffened cylinder in axial compression. Donnell's equations were used for the shell and Vlasov's thin-walled beam theory for the stiffeners. In this way it was possible to treat stiffeners as beams of arbitrary cross section.

Syngellakis and Walker[5] presented an analysis of the critical and post-critical behaviour of sparsely stringer-stiffened cylinders, where the stiffeners were treated as narrow plates. The solution procedure was considerably simplified by introducing a number of assumptions consistent with experimental observations. It was then shown that such shells have several critical loads in close proximity, a feature which could result in the coupling of modes in the post-critical range and led to an increase in imperfection-sensitivity. Initial post-critical paths for each of the critical loads were shown to be either stable or unstable, depending on the shell geometry.

In a later paper, Syngellakis and Walker[6] extended their earlier analysis by considering the effects of geometric imperfections. In the earlier paper, the critical mode was assumed to be symmetric about a panel mid-generator, and antisymmetric about a stiffener. The later paper[6] assumed an initial imperfection of the same form, and established the imperfection sensitivity characteristics of buckling into an eigenmode that was asymmetric about the panel mid-generator.

In the plastic range, the only work related to stiffened cylinders appears to be that of Tvergaard[7], who extended Koiter's[2] analysis of a simply supported panel into the plastic range. Tvergaard's analysis included an asymptotic analysis of the initial post-critical behaviour and imperfection-sensitivity of an equivalent "hypoelastic" panel (i.e. with the elastic unloading

branch of the stress–strain curve suppressed), as well as a numerical study of imperfection-sensitivity of the actual panel.

In the present paper the bifurcation of an elastic–plastic discretely stringer-stiffened cylinder in axial compression is considered.

The analysis is essentially an extension of that of Ref. [5], in that we treat a shell which has an even number of equally-spaced longitudinal stiffeners, which are modelled as flat plates. The aim of this work is, firstly, to provide an analysis which will complement earlier elastic analyses. The results presented later should give an idea of the circumstances under which it can be expected that bifurcation will take place after the onset of plasticity; in particular, the main body of the results will centre of the effects of stiffener size on critical stresses, for both elastic and elastic–plastic shells.

When the critical stress $\sigma_{st}$ of a stiffener, treated as a long plate simply supported on three edges and free along one longitudinal edge, is much lower than the critical stress $\sigma_{panel}$ of a simply-supported cylindrical panel, the critical stress $\sigma_c$ of the stiffened shell is expected to be reduced to a value below that of $\sigma_{panel}$.

We shall discuss this phenomenon in greater detail for internally-stiffened shells, in order to show more clearly how the critical stress varies with stiffener size. It will be argued that this consideration may become more important if efforts to optimise the design of stiffened shells are increasingly directed towards optimisation with respect to the slenderness of stiffeners. Furthermore, in these circumstances the results of Koiter [2] and Tvergaard [7] may be misleading, inasmuch as a very low torsional rigidity of the stiffeners could result in a critical stress $\sigma_c$ significantly less than $\sigma_{panel}$, because of the destablising influence of the stiffeners.

This is contrary to the implications from Refs. [2,7] that shells having stiffeners with low torsional rigidity may be treated as an assemblange of simply-supported panels; this would then yield a critical stress equal to $\sigma_{panel}$. Results presented will also include a comparison of critical stresses of shells with inside stiffening, with those having outside stiffeners.

## 2. THE SHELL MODEL

Consider the stiffened shell in Fig. 1, which consists of a circular cylinder with an *even* number of equally spaced longitudinal stiffeners. The shell has radius $r$, wall-thickness $t$, and length $l$, while each stiffener has depth $2d$ and thickness $t_s$. Furthermore, the width of each panel is given by the angle $2\theta_0$: that is,

$$\theta_0 = \pi/N, \tag{1}$$

where $N$ is the number of stiffeners. The coordinates of the $i$th panel midsurface are $(x^1, x^2) = (x, \theta^{(i)})$ and the coordinate $z$ measures distances outward from the panel mid-surface. The coordinates of a typical stiffner are $(X_1, X_2) = (x, y)$, as shown in Fig. 1: each stiffner is considered to be a flat plate with midsurface in the $(X_1, X_2)$ plane, and distances normal to the midsurface are measured by the coordinate $Z$. The centroid of a stiffner is in general a distance $y = e$ from the shell midsurface; so, for a shell that is internally stiffened, we have

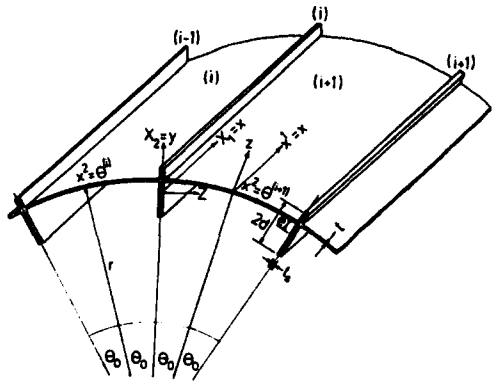


Fig. 1. Geometry of stiffened shell.

$$e = d - t/2. \tag{2}$$

The shell is subjected to a uniform axial compressive stress $\sigma_x$, applied over the end areas of the panels and stiffeners.

## 3. KINEMATICAL CONSIDERATIONS

The displacements of the shell midsurface are $u^\alpha$ in the direction of the surface base vectors, and $w$ in the direction of the outward unit normal; the inplane stiffener displacements are $U_\alpha$, referred to the $(X_1, X_2)$ axes, and $W$ normal to the stiffener midsurface. Here Greek sub- and superscripts range from 1 to 2.

In the following the strain-displacement relations of Donnell–Mushtari–Vlasov shell theory are used for the panels; these are

$$\epsilon_{\alpha\beta} = \frac{1}{2}(u_{\alpha;\beta} + u_{\beta;\alpha}) - b_{\alpha\beta}w + \frac{1}{2}(w_{,\alpha}\, w_{,\beta}) \tag{3}$$

$$\kappa_{\alpha\beta} = w_{;\alpha\beta} \tag{4}$$

where $(\,)_{;\alpha}$ denotes covariant differentiation and $(\,)_{,\alpha}$ partial differentiation with respect to $\alpha$. $\epsilon_{\alpha\beta}$ and $\kappa_{\alpha\beta}$ are the midsurface membrane and bending strain tensors, and $b_{\alpha\beta}$ is the curvature tensor for the undeformed midsurface. For a typical stiffener, the membrane and bending strain tensors $E_{\alpha\beta}$ and $K_{\alpha\beta}$ are

$$E_{\alpha\beta} = \frac{1}{2}(U_{\alpha,\beta} + U_{\beta,\alpha}) + \frac{1}{2}\, W_{,\alpha} W_{,\beta} \tag{5}$$

$$K_{\alpha\beta} = W_{;\alpha\beta}; \tag{6}$$

these quantities are referred to the rectangular axes of the stiffener. Furthermore, the strain tensor $\eta_{\alpha\beta}$ is related to the membrane and bending strain tensors by

$$\eta_{\alpha\beta} = \epsilon_{\alpha\beta} - z\kappa_{\alpha\beta} \quad \text{in the shell,} \tag{7}$$

$$\eta_{\alpha\beta} = \mathrm{E}_{\alpha\beta} - \mathrm{Z}\mathrm{K}_{\alpha\beta} \text{ and in the stiffeners.} \tag{8}$$

The condition of continuity of displacements (physical components) and slopes at the $i$th stiffener-panel junction is expressed as

$$\begin{aligned} u^{(i)}(x, \theta_0) &= U^{(i)}(x, e) = u^{(i+1)}(x, -\theta_0) \\ v^{(i)}(x, \theta_0) &= W^{(i)}(x, e) = v^{(i+1)}(x, -\theta_0) \\ w^{(i)}(x, \theta_0) &= V^{(i)}(x, e) = w^{(i+1)}(x, -\theta_0) \\ \frac{1}{r} w^{(i)}_{,\theta}(x, \theta_0) &= -W^{(i)}_{,y}(x, e) = \frac{1}{r} w^{(i+1)}_{,\theta}(x, -\theta_0). \end{aligned} \tag{9}$$

Following Syngellakis and Walker[5], we assume that the stiffener cross sections remain straight and normal to the shell; in other words, that

$$\begin{aligned} U^{(i)}(x, y) &= u^{(i)}(x, \theta_0) - (y - e) w^{(i)}_{,x}(x, \theta_0) \\ V^{(i)}(x, y) &= w^{(i)}(x, \theta_0) \\ W^{(i)}(x, y) &= v^{(i)}(x, \theta_0) - \frac{1}{r}(y - e) w^{(i)}_{,\theta}(x, \theta_0) \end{aligned} \tag{10}$$

for the $i$th stiffener. Hereafter the $(i)$ superscripts will be omitted when it is obvious that we are referring to a typical panel or stiffener.

## 4. CONSTITUTIVE RELATIONS

The three-dimensional stress-increments $\sigma^{ij}$ and strain increments $\eta_{kl}$ are linearly related by

$$\dot{\sigma}^{ij} = \bar{C}^{ijkl}\dot{\eta}_{kl}. \tag{11}$$

Two small strain theories of plasticity are used. For $J_2$ flow theory, the instantaneous moduli $\bar{C}^{ijkl}$ are

$$\bar{C}^{ijkl} = \frac{E}{1+\nu}\left[\frac{1}{2}(g^{ik}g^{jl}+g^{il}g^{jk})+\frac{\nu}{1-2\nu}g^{ij}g^{kl}-\frac{h_1 S^{ij}S^{kl}}{1+\nu+2h_1J_2}\right] \tag{12}$$

where

$$S^{ij} = \sigma^{ij} - \frac{1}{3}g^{ij}g_{kl}\sigma^{kl}$$

$$J_2 = \frac{1}{2}g_{ik}g_{jl}\sigma^{ij}\sigma^{kl}$$

and $g_{ij}$ is the metric tensor of the shell (equal to the Kronecker delta in the case of the stiffeners). The function $h_1(J_2)$ is determined from the tensile stress–strain curve in terms of the tangent modulus $E_t$, as

$$\begin{aligned} h_1 &= 3(E/E_t - 1)/(4J_2) \quad \text{for} \quad J_2 = (J_2)_{\max} \text{ and } \dot{J}_2 \geq 0 \\ &0 \quad \text{for} \quad J_2 < (J_2)_{\max} \text{ or } \dot{J}_2 < 0. \end{aligned} \tag{13}$$

Secondly, for $J_2$ deformation theory,

$$\bar{C}^{ijkl} = \frac{E}{1+\nu+h_2}\left[\frac{1}{2}(g^{ik}g^{jl}+g^{il}g^{jk})+\frac{3\nu+h_2}{3(1-2\nu)}g^{ij}g^{kl}-\frac{h_2' S^{ij}S^{kl}}{1+\nu+h_2+2h_2'J_2}\right] \tag{14}$$

where $h_2(J_2) = 3(E/E_s - 1)/2$ and is found from the tensile stress–strain curve; $E_s$ is the secant modulus and $h_2' = dh_2/dJ_2$.

Uniaxial behaviour is represented by the following piecewise power law

$$\epsilon = \begin{cases} \sigma/E & \text{for } \sigma \leq \sigma_y \\ \sigma_y/E[(\sigma/\sigma_y)^n/n + (n-1)/n] & \text{for } \sigma > \sigma_y \end{cases} \tag{15}$$

in which the tangent modulus is continuous at the yield stress and $n$ is the strain-hardening exponent.

The usual assumption of a state of approximate plane stress in the shell and stiffeners gives

$$\dot{\sigma}^{\alpha\beta} = C^{\alpha\beta\kappa\gamma}\dot{\eta}_{\kappa\gamma} \tag{16}$$

where Greek indices range from 1 to 2, and the plane-stress moduli $C^{\alpha\beta\kappa\gamma}$ are found from

$$C^{\alpha\beta\kappa\gamma} = \bar{C}^{\alpha\beta\kappa\gamma} - \bar{C}^{\alpha\beta 33}\bar{C}^{33\kappa\gamma}/\bar{C}^{3333}. \tag{17}$$

Bending moment and stress resultant tensors are defined by

$$\begin{aligned} n^{\alpha\beta} &= \int_{-t/2}^{t/2}\sigma^{\alpha\beta}\,dz, \qquad m^{\alpha\beta} = \int_{-t/2}^{t/2}\sigma^{\alpha\beta}z\,dz \\ N^{\alpha\beta} &= \int_{-t_s/2}^{t_s/2}\sigma^{\alpha\beta}\,dZ, \quad M^{\alpha\beta} = \int_{-t_s/2}^{t_s/2}\sigma^{\alpha\beta}Z\,dZ. \end{aligned} \tag{18}$$

Birfurcation is assumed to take place from a membrane prebuckling state of uniform axial compressive stress. Now, for bifurcation to occur at the lowest eigenvalue, it is necessary that no elastic unloading takes place. The unloading branch, represented by the second of the stress–strain relations (13), must therefore be suppressed in the case of the flow theory. Under these conditions the use of (7, 8, 16) in the rate of form of (18) gives the following relationships between physical components of stress-resultant rates, and membrane and bending strain rates:

$$\begin{bmatrix} \dot{n}_x \\ \dot{n}_\theta \\ \dot{n}_{x\theta} \end{bmatrix} = Et \begin{bmatrix} C_{11} & C_{12} & 0 \\ C_{12} & C_{22} & 0 \\ 0 & 0 & C_{33} \end{bmatrix} \begin{bmatrix} \dot{\epsilon}_x \\ \dot{\epsilon}_\theta \\ \dot{\gamma}_{x\theta} \end{bmatrix}, \quad \begin{bmatrix} \dot{m}_x \\ \dot{m}_\theta \\ \dot{m}_{x\theta} \end{bmatrix} = \frac{Et^3}{12} \begin{bmatrix} C_{11} & C_{12} & 0 \\ C_{12} & C_{22} & 0 \\ 0 & 0 & 2C_{33} \end{bmatrix} \begin{bmatrix} \dot{\kappa}_x \\ \dot{\kappa}_\theta \\ \dot{\kappa}_{x\theta} \end{bmatrix} \tag{19}$$

where, for $J_2$ flow theory,

$$\begin{aligned} C_{11} &= (E/E_t + 3)/4D \\ C_{12} &= (E/E_t + 2\nu - 1)/2D \\ C_{22} &= (E/E_t)/D \\ C_{33} &= 1/2(1+\nu) \\ D &= 1/4\{(5-4\nu)E/E_t - (1-2\nu)^2\} \end{aligned} \tag{20}$$

and, for $J_2$ deformation theory,

$$\begin{aligned} C_{11} &= (E/E_t + 3E/E_s)/4D \\ C_{12} &= (E/E_t + 2\nu - 1)/2D \\ C_{22} &= (E/E_t)/D \\ C_{33} &= [2(1+\nu)(1+3(E/E_s - 1)/2(1+\nu)\}]^{-1} \\ D &= \{(3E/E_s + 2 - 4\nu)E/E_t - (1-2\nu)^2\}/4. \end{aligned} \tag{21}$$

For the stiffeners, the corresponding stiffener quantities appear in (19), and $t$ is replaced by $t_s$. The usual elastic coefficients are recovered by setting $E_t = E$ in (20).

## 5. CRITERION FOR BIFURCATION

To find the stress $\sigma_c$ at which bifurcation occurs, the uniqueness criterion given by Hutchinson[8] for DMV shell theory is used: that is, for the functional $F$, given by

$$F = \sum_{i=1}^{N} \left\{ \int_{A_p^{(i)}} (\tilde{m}^{\alpha\beta}\tilde{\kappa}_{\alpha\beta} + \tilde{n}^{\alpha\beta}\tilde{\epsilon}_{\alpha\beta} + n_0{}^{\alpha\beta}\tilde{w}_{,\alpha}\tilde{w}_{,\beta})\, dA_p^{(i)} + \int_{A_s^{(i)}} (\tilde{M}^{\alpha\beta}\tilde{K}_{\alpha\beta} + \tilde{N}^{\alpha\beta}\tilde{E}_{\alpha\beta} + N_0{}^{\alpha\beta}\tilde{W}_{,\alpha}\tilde{W}_{,\beta})\, dA_s^{(i)} \right\} \tag{22}$$

the condition

$$F > 0$$

is sufficient to ensure uniqueness of the solution increment at any stage of the loading programme. Here a tilde (~) superscript denotes the difference between increments on the fundamental path and those on the bifurcated path, and summation is over all panels and stiffeners. For bifurcation to be possible at the lowest eigenvalue, it is necessary that no elastic unloading occurs; $F$ then attains a zero minimum, and the eigenvalue problem can be stated as

$$\delta F = 0 \tag{23}$$

subject to the constitutive relations, eqns (19), and the compatibility conditions, eqns (3)–(6). The variational eqn (23) then becomes, in terms of physical components,

$$\sum_{i=1}^{N}\Big\{\int_{A_p^{(i)}}(\tilde{m}_x\delta\tilde{\kappa}_x+2\tilde{m}_{x\theta}\delta\tilde{\kappa}_{x\theta}+\tilde{m}_\theta\delta\tilde{\kappa}_\theta+\tilde{n}_x\delta\tilde{\epsilon}_x+2\tilde{n}_{x\theta}\delta\tilde{\epsilon}_{x\theta}$$

$$+\tilde{n}_\theta\delta\tilde{\epsilon}_\theta+\sigma_c t\tilde{w}_{,x}\delta\tilde{w}_{,x})\,dA_p^{(i)}+\int_{A_s^{(i)}}(\tilde{M}_x\delta\tilde{K}_x+2\tilde{M}_{xy}\delta\tilde{K}_{xy} \tag{24}$$

$$+\tilde{M}_y\delta K_y+\tilde{N}_x\delta\tilde{E}_x+2\tilde{N}_{xy}\delta\tilde{E}_{xy}+\tilde{N}_y\delta\tilde{E}_y+\sigma_c t_s\tilde{W}_{,x}\tilde{W}_{,x})\,dA_s^{(i)}\Big\}=0.$$

Substitution of the strain-displacement relations into these variational quantities and use of the divergence theorem in the usual way, requires that the equations

$$\tilde{n}_{x,x}+(1/r)\tilde{n}_{x\theta,\theta}=0 \tag{25}$$

$$\tilde{n}_{x\theta,x}+(1/r)\tilde{n}_{\theta,\theta}=0 \tag{26}$$

$$\tilde{m}_{x,x}+(2/r)\tilde{m}_{x\theta,x\theta}+(1/r^2)\tilde{m}_{\theta,\theta\theta}+\tilde{n}_\theta/r-\sigma_c t\tilde{w}_{,xx}=0 \tag{27}$$

be satisfied for each panel, and that on the boundaries the line integrals satisfy the conditions

$$\sum_{i=1}^{N}\Big\{\int_{-\theta_0}^{\theta_0}\{\tilde{n}_x\delta u+\tilde{n}_{x\theta}\delta\tilde{v}+\tilde{m}_x\delta\tilde{w}_{,x}+(\sigma_c t\tilde{w}_{,x}-\tilde{m}_{x,x}-2\tilde{m}_{x\theta,\theta}/r)\delta\tilde{w}\}]_{x=0}^{x=\ell}r\,d\theta^{(i)}$$

$$+\int_0^\ell\{\tilde{n}_{x\theta}\delta\tilde{u}+\tilde{n}_\theta\delta\tilde{v}-(\tilde{m}_{\theta,\theta}/r+2\tilde{m}_{x\theta,x})\delta\tilde{w}+\tilde{m}_\theta\delta\tilde{w}_{,\theta}/r\}]_{\theta^{(i)}=-\theta_0}^{\theta^{(i)}=\theta_0}dx$$

$$+(2/r)[\tilde{m}_{x\theta}\delta\tilde{w}]_{x=0}^{x=\ell}]_{\theta^{(i)}=-\theta_0}^{\theta^{(i)}=\theta_0}$$

$$-\int_0^\ell\int_{-d}^{d}\{(\tilde{N}_{x,x}+\tilde{N}_{xy,y})\delta\tilde{U}+(\tilde{N}_{xy,x}+\tilde{N}_{y,y})\delta\tilde{V}+(\sigma_c t_s\tilde{W}_{,xx}-\tilde{M}_{x,xx}$$

$$-2\tilde{M}_{xy,xy}-\tilde{M}_{y,yy})\delta\tilde{W}]]_{\theta^{(i)}=-\theta_0}dy\,dx$$

$$+\int_0^\ell\{\tilde{N}_{xy}\delta\tilde{U}+\tilde{N}_y\delta\tilde{V}+\tilde{M}_y\delta\tilde{W}_{,y}-(2\tilde{M}_{xy,x}+\tilde{M}_{y,y})\delta\tilde{W}]]_{y=-d}^{y=d}]_{\theta^{(i)}=-\theta_0}dx$$

$$+2[\tilde{M}_{xy}\delta\tilde{W}]_{y=-d}^{y=d}]_{x=0}^{x=\ell}]_{\theta^{(i)}=-\theta_0}\Big\}=0. \tag{28}$$

The stiffener variational displacements in (28) may be written in terms of panel variational displacements, using (10). A set of boundary conditions are then extracted from (28); these are given in the Appendix.

With the aid of the constitutive equations and following Storåkers [9] eqns (25)–(27) may be written in terms of displacement rates, in the uncoupled forms

$$L\tilde{u}=C_{22}\tilde{w}_{,\xi\theta\theta}-C_{12}\tilde{w}_{,\xi\xi\xi} \tag{29}$$

$$L\tilde{v}=-(1/C_{33})(C_{11}C_{22}-C_{12}^2-C_{12}C_{33})\tilde{w}_{,\xi\xi\theta}-C_{22}\tilde{w}_{,\theta\theta\theta} \tag{30}$$

$$(C_{11}C_{22}-C_{12}^2)\tilde{w}_{,\xi\xi\xi\xi}+L[(t^2/12r^2)L'(\tilde{w})-(\sigma_c/E)\tilde{w}_{,\xi\xi}]=0 \tag{31}$$

where

$$L(\,)=C_{11}(\,)_{,\xi\xi\xi\xi}+(1/C_{33})(C_{11}C_{22}-C_{12}^2-2C_{12}C_{33})(\,)_{,\xi\xi\theta\theta}+C_{22}(\,)_{,\theta\theta\theta\theta}$$

$$L'(\,)=C_{11}(\,)_{,\xi\xi\xi\xi}+2(C_{12}+2C_{33})(\,)_{,\xi\xi\theta\theta}+C_{22}(\,)_{,\theta\theta\theta\theta}$$

and where the dimensionless coordinate $\xi=x/r$.

As in Ref. [5] it is assumed that the eigenmode of radial displacement $\tilde{w}$ is symmetric about the mid-generator of a panel, and antisymmetric about a stiffener. Such an assumption is supported by experimental observations of tests carried out on sparsely stiffened cylinders [10].

The assumption of antisymmetry, together with the compatibility conditions (9) result in the longitudinal edge requirement

$$\tilde{w}(\xi, \theta_0) = 0 \tag{32}$$

for each panel.

A separated solution to eqn (31) is now sought in the form

$$\tilde{w} = \sin \alpha\xi \exp(\bar{\beta}\theta) \tag{33}$$

for a typical panel where $\alpha = m\pi r/\ell$, and $m$ is the number of longitudinal half-waves. The characteristic equation is

$$(C_{11}C_{22} - C_{12}^2)\alpha^4 + \left\{C_{11}\alpha^4 + \frac{C_{11}C_{22} - C_{12}^2 - 2C_{12}C_{33}}{C_{33}}\alpha^2\bar{\beta}^2 + C_{22}\bar{\beta}^4\right\}\left\{\frac{t^2}{12r^2}\right.$$

$$\left.(C_{11}\alpha^4 + 2(C_{12} + 2C_{33})\alpha^2\bar{\beta}^2 + C_{22}\bar{\beta}^4) + \frac{\sigma_c}{E}\alpha^2\right\} = 0. \tag{34}$$

Making use of the condition of symmetry of $\tilde{w}$ about $\theta = 0$, we find that there are four distinct roots of $\bar{\beta}$; for the $i$th panel, therefore,

$$\tilde{w} = \sin \alpha\xi \sum_{j=1}^{4} A_j \cos \beta_j\theta \tag{35}$$

where $\beta_j = i\bar{\beta}_j$, $i = \sqrt{-1}$, and the $A_j$ are constants, in general complex. Equations (29) and (30) may now be solved, using (35), to yield

$$\tilde{u} = \cos \alpha\xi \sum_{j=1}^{4} A_j\mu_{1j} \cos \beta_j\theta \tag{36}$$

$$\tilde{v} = -\sin \alpha\xi \sum_{j=1}^{4} A_j\beta_j\mu_{2j} \sin \beta_j\theta \tag{37}$$

where

$$\mu_{1j} = (C_{12}\alpha^3 - C_{22}\alpha\beta_j^2)/\left\{C_{11}\alpha^4 + \frac{1}{C_{33}}(C_{11}C_{22} - C_{12}^2 - 2C_{12}C_{33})\alpha^2\beta_j^2 + C_{22}\beta_j^4\right\}$$

$$\mu_{2j} = \frac{\left\{\frac{1}{C_{33}}(C_{11}C_{22} - C_{12}^2 - C_{12}C_{33})\alpha^2 + C_{22}\beta_j^2\right\}}{\left\{C_{11}\alpha^4 + \frac{1}{C_{33}}(C_{11}C_{22} - C_{12}^2 - 2C_{12}C_{33})\alpha^2\beta_j^2 + C_{22}\beta_j^4\right\}}$$

The solutions (35)–(37) identically satisfy the boundary conditions

$$\tilde{u}_{,\xi} = \tilde{v}_{,\theta} = \tilde{w} = w_{,\xi\xi} = \tilde{w}_{,\theta\theta} = 0 \quad \text{at} \quad \xi = 0,\ \ell/r:$$

$$\tilde{v} = \tilde{v}_{,\xi\xi} = \tilde{w} = \tilde{w}_{,\theta} = \tilde{w}_{,\theta\xi\xi} = 0 \quad \text{at} \quad \xi = 0,\ \ell/r \quad \text{and} \quad \theta^{(i)} = \theta_0.$$

These can be seen to satisfy conditions (i)–(iv) and (x)–(xv) in the Appendix. It therefore remains to satisfy the conditions (v)–(ix).

Now, from the assumption of antisymmetry of $\tilde{w}$ about a stiffener,

$$\sum A_j^{(i)} \cos \beta_j\theta^{(i)} = -\sum A_j^{(i+1)} \cos \beta_j\theta^{(i+1)} \tag{38}$$

and therefore

$$A_j^{(i)} = -A_j^{(i+1)} \tag{39}$$

From (36), it can be seen that $\bar{u}$, like $\bar{w}$, is symmetric about a panel mid-generator and antisymmetric about a stiffener (from 39). Along the $i$th stiffener, therefore, $\bar{u}$ and $\bar{w}$ are set equal to zero.

The boundary conditions at the $i$th panel-stiffener junction ($\theta^{(i)} = \theta_0$) are

$$\bar{u} = 0 \tag{40}$$

$$\bar{w} = 0 \tag{41}$$

which satisfy boundary conditions (v), (vii) and (ix); after some simplification, (vi) and (viii) become

$$[C_{12}\bar{u}_{,\xi} + C_{22}(\bar{v}_{,\theta} + \bar{w})]_{-\theta_0^{(i)}}^{\theta_0^{(i)}} + 2\frac{b}{r}\frac{t_s}{t}\left\{\left(C_{11}\bar{v} + C_{11}\frac{e}{r}\bar{w}_{,\theta}\right)_{,\xi\xi\xi\xi}\left(\frac{t_s}{t}\right)^2\left(\frac{t^2}{12r^2}\right)\right.$$
$$\left. - \frac{\sigma_c}{E}\left(\bar{v} + \frac{e}{r}\bar{w}_{,\theta}\right)_{,\xi\xi}\right\} = 0 \tag{42}$$

$$\frac{t^2}{12r^2}[C_{12}\bar{w}_{,\xi\xi} + C_{22}\bar{w}_{,\theta\theta}]_{-\theta_0^{(i)}}^{\theta_0^{(i)}} + 2\frac{b}{r}\frac{t_s}{t}\left\{\left(\frac{t_s}{t}\right)^2\left(\frac{t^2}{12r^2}\right)\left(C_{11}\left(\bar{v}\frac{e}{r} + \frac{b^2/3 + e^2}{r^2}\bar{w}_{,\theta}\right)_{,\xi\xi\xi\xi}\right.\right.$$
$$\left.\left. - 4C_{33}\bar{w}_{,\xi\xi\theta}\right) - \frac{\sigma_c}{E}\left\{\frac{e}{r}\bar{v}_{,\xi\xi} + \frac{b^2/3 + e^2}{r^2}w_{,\xi\xi\theta}\right)\right\} = 0. \tag{43}$$

Substitution of (35)–(37) and (39) into (40)–(43) yields the set of homogeneous linear equations in $A_j$

$$\sum A_j\mu_{ij}\cos\beta_j\theta_0 = 0 \tag{44}$$

$$\sum A_j\cos\beta_j\theta_0 = 0 \tag{45}$$

$$\sum A_j\{C_{22}(\mu_{2j}\beta_j^2 - 1) + C_{12}\alpha\mu_{1_\mu}\}\cos\beta_j\theta_0 + \alpha^2\frac{bt_s}{rt}\left\{\frac{\sigma_c}{E} + \frac{t_s^2}{12r^2}C_{11}\alpha^2\right\}\sum A_j\beta_j(\mu_{2j} + e/r)\sin\beta_j\theta_0 = 0 \tag{46}$$

$$\frac{t^2}{12r^2}\sum A_j(C_{12}\alpha^2 + C_{22}\beta_j^2)\cos\beta_j\theta_0 + \frac{bt_s}{rt}\alpha^2\sum A_j\beta_j\left[\alpha^2\frac{bt_s}{rt}\left\{\frac{\sigma_c}{E} + C_{11}(t_s^2/12r^2)\alpha^2\right\}\left\{\frac{e}{r}\mu_{2j}\right.\right.$$
$$\left.\left. + \frac{e^2 + b^2/3}{r^2}\right\} + 4C_{33}\alpha^2 t_s^2/12r^2\right]\sin\beta_j\theta_0 = 0 \tag{47}$$

which can be written in matrix form as

$$M\{A\} = 0. \tag{48}$$

A non-trivial solution for $A_j$ can then be found for a particular value of $\alpha$ once the roots $\beta_j$ have been found from (34) for a chosen value of $\sigma_c/E$. An iterative process is then employed to find the value of $\sigma_c/E$ at which det ($M$) in (48) vanishes. The process may then be repeated to find the least eigenvalue and corresponding eigenmode. Because of the simplifying assumptions made, it has only been necessary to solve the equilibrium equations for a typical panel, and to satisfy the boundary conditions along a typical stiffener.

## 6. PRESENTATION OF RESULTS

Figure 2 shows a typical plot of critical stress $\sigma_c$ vs log ($\alpha$), where $\sigma_c$ is normalised with respect to the classical critical stress of an elastic unstiffened cylinder $\sigma_{cu}$; this stress is given by

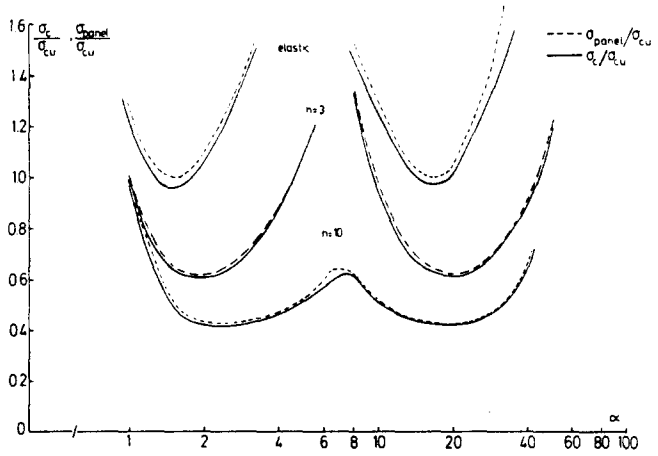


Fig. 2. Critical stresses $\sigma_c$ and $\sigma_{panel}$ for stiffened shell and equivalent panel, respectively; $r/t = 100$, internally stiffened with 10 stiffeners having $d/t = 5$, $d/t_s = 10$. Curves are for elastic materials, and elastic-plastic materials (flow theory) having $\sigma_y/E = 0.002$.

$$\sigma_{cu} = -Et/r\sqrt{(3(1-\nu^2))}. \tag{49}$$

The shell radius-thickness ratio is $r/t = 100$, there are 10 stiffeners, and the stiffener geometry is specified by $d/t_s = 10$, $t_s/r = 0.005$; the shell is internally stiffened. Curves are drawn for an elastic material, and for elastic–plastic materials having a yield stress $\sigma_y/E$ of 0.002, and strain-hardening exponents of $n = 3$ and 10 (high and low strain-hardening, respectively). Also shown in the figure are curves corresponding to the stresses of elastic and elastic–plastic simply-supported panels of the same width as the panels of the stiffened shell. These results were found from Timoshenko and Gere[11] and from Tvergaard's[7] analysis. For this geometry the least critical stresses are all quite close to those for simply-supported panels having the same width as the panels in the stiffened shell.

(a) *Effect of stiffener size*

In this section we present some results which show the effects of stiffener size on an internally-stiffened shell. Of particular interest is the possible detrimental effect of very slender stiffeners, as mentioned briefly by Syngellakis and Walker[6]; we shall examine these effects more closely, for elastic as well as elastic–plastic shells.

Consider first the following: a long axially compressed plate such as one of the stiffeners, when simply-supported on three sides and free along one of the longitudinal edges, has a critical stress $\sigma_{st}$ proportional to (thickness/breadth)$^2$ in the elastic range. This is close to that of an axially compressed cruciform column whose flanges have the same dimensions as the plate[11]. If the width is $2d$ and the thickness $t_s$, then the respective stresses in the elastic range are

$$\sigma_{st} = -\frac{0.75}{1-\nu} G\,(t_s/2d)^2, \qquad \sigma_{cruc} = -G(t_s/2d)^2 \tag{50}$$

where $G = E/2(1+\nu)$ is the elastic shear modulus. For a value of $\nu$ of 0.3, the two stresses differ by 7%. In the plastic range, the value of $\sigma_{cruc}$ is the same as the elastic value, eqn $(50)_2$, if flow theory is used[12]. An analysis of the corresponding plate problem would show that the flow theory stress is also practically equal to the elastic value of $\sigma_{st}$. With the use of deformation theory, though, the values of $\sigma_{st}$ and $\sigma_{cruc}$ can be significantly reduced[12].

In Figs. 3 the least critical stress $\sigma_c$ of an internally stiffened shell is plotted vs $d/t$, with the value of $d/t_s$ held constant in each of the figures. The shell has radius-thickness ratio $r/t = 100$, and 10 stiffeners. Therefore, in each figure $\sigma_{st}$ is a constant, while the increase in $d/t$ along the horizontal axis may be interpreted as a increase in stiffener size. This is depicted in Figs. 3, below the corresponding graphs. The values of $\sigma_{panel}$, the least critical stress of a simply supported panel with the same dimensions as a panel in the stiffened shell, are shown in the figures, as are the values of $\sigma_{st}$.

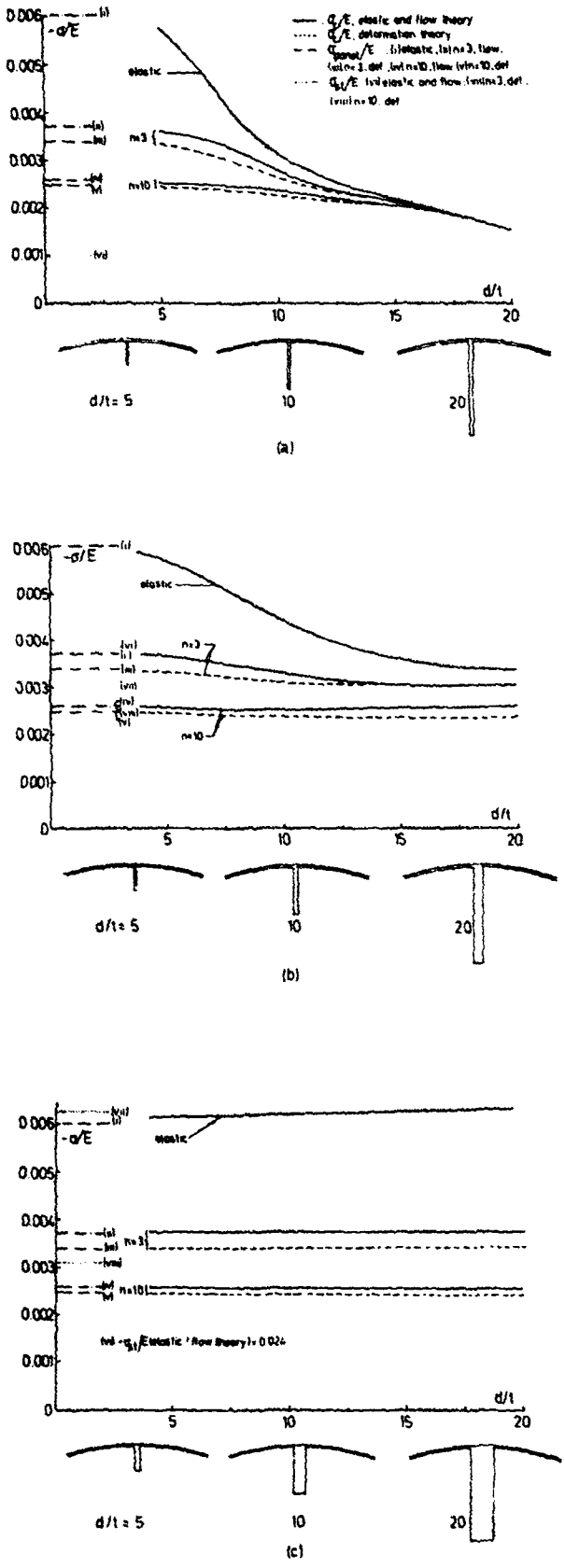


Fig. 3. Critical $\sigma_c$ for stiffened shell vs $d/t$, for $d/t_s = 10$(a); 5 (b); 2 (c). For elastic–plastic materials, $\sigma_y/E = 0.002$. Values of $\sigma/E$ marked (i)–(viii) represent least critical stress $-\sigma_{panel}/E$ and $-\sigma_{st}/E$ for elastic and elastic–plastic materials.

For $d/t_s = 10$, Fig. 3(a), $\sigma_{st} \ll \sigma_{panel}$. Here $\sigma_c$ decreases with an increase in $d/t$ for the elastic and elastic–plastic (flow theory) cases, from a value close to $\sigma_{panel}$ to a value approaching $\sigma_{st}$. For $d/t_s = 5$, Fig. 3(b), $\sigma_{st} < \sigma_{panel}$ in the elastic range, and we see the same behaviour as in Fig. 3(a). For elastic–plastic shells (flow theory), $\sigma_{st} \simeq \sigma_{panel}$ for $n = 3$, and $\sigma_{st} > \sigma_{panel}$ $n = 10$.

Here $\sigma_c$ for the stiffened shell decreases for $n = 3$, and remains virtually constant for $n = 10$. Finally, for $d/t_s = 2$, Fig. 3(c), $\sigma_{st}$ is very high and we see that $\sigma_c$ is slightly greater than $\sigma_{panel}$, and virtually constant, for all materials.

These results may be summarised as follows: when $\sigma_{st} < \sigma_{panel}$, the critical stress of the stiffened shell decreases from $\simeq \sigma_{panel}$ to $\simeq \sigma_{st}$ over the range of $d/t$ considered (see Fig. 3(a), all cases; 3(b), elastic). When $\sigma_{st} \simeq \sigma_{panel}$, the critical stress of the stiffened shell decreases slightly (see Fig. 3(b), $n = 3$). When $\sigma_{st} > \sigma_{panel}$, the critical stress of the stiffened shell remains close to the value of $\sigma_{panel}$. As far as the results for deformation theory go, similar conclusions apply, this time with respect to the values of $\sigma_{st}$, $\sigma_{panel}$ and $\sigma_c$ found using deformation theory.

It is necessary to point out at this stage that the results for low values of $d/t$ should be subject to further investigation. The assumptions which were made regarding the mode of buckling deformation (e.g. $\bar{w} = 0$ along a panel-stiffener junction) are not necessarily applicable for such a case, as an overall buckling mode (i.e. half-waves extending circumferentially over a number of stiffeners) is clearly possible.

The above results contrast with those of Koiter[2] and Tvergaard[7]. These authors have given results for simply-supported panels which form part of a stiffened shell, whose stiffeners have negligible torsional ridigity. According to these analyses, the stiffened shell which we have considered should have a critical stress close to $\sigma_{panel}$, when the torsional stiffness of the stiffeners is low.

However, when the stiffeners have low torsional rigidity, i.e. when $\sigma_{st} \ll \sigma_{panel}$, the critical stress of the stiffened shell can be reduced to a value significantly lower than $\sigma_{panel}$. In particular, returning to Fig. 3(a), as the stiffener size increases relative to the shell with $\sigma_{st}$ remaining constant, the value of $\sigma_c$ decreases. An interpretation of behaviour is that, as the stiffener size increases, the resistance to deformation of a stiffener provided by the adjacent panels becomes relatively smaller, and so the composite shell buckles at a stress which approaches $\sigma_{st}$. Therefore, in the design of such a stiffened shell, one would have to weigh the advantage of an increase in bending stiffness in the axial direction, against the possibility of destabilization due to the slenderness (and therefore low torsional rigidity) of the stiffeners. When $\sigma_{st} \gg \sigma_{panel}$, as in Fig. 3(c), the relatively low value of $\sigma_{panel}$ governs the critical stress of the stiffened shell. The value of $\sigma_{panel}$ could, of course, be raised by making the panels narrower, i.e. by increasing the number of stiffeners, This can be seen in Table 1; here, as the number of stiffeners increases, $\sigma_{panel}$ increases. Furthermore, $\sigma_{st} \gg \sigma_{panel}$ and the value of $\sigma_c$ is

Table 1. Dimensionless critical stresses $S_{(\ldots)} = \sigma_{(\ldots)}/\sigma_{cu}$ for an internally-stiffened shell with $r/t = 100$, $d/t_s = 2$, $d/t = 10$; $\sigma_y/E = 0.002$ for elastic–plastic materials

| No.of Stiffeners | | 10 | 20 | 30 |
|---|---|---|---|---|
| Elastic | $S_{st}$ | 3.967 | 3.967 | 3.967 |
| | $S_{panel}$ | 1.000 | 1.018 | 1.549 |
| | $S_c$ | 1.023 | 1.443 | 2.586 |
| n=3 (flow theory) | $S_{st}$ | 3.967 | 3.967 | 3.967 |
| | $S_{panel}$ | 0.618 | 0.821 | 1.307 |
| | $S_c$ | 0.621 | 0.959 | 1.777 |
| n=3 (def.theory) | $S_{st}$ | 1.033 | 1.033 | 1.033 |
| | $S_{panel}$ | 0.557 | 0.625 | 0.749 |
| | $S_c$ | 0.570 | 0.793 | 0.889 |
| n=10 (flow theory) | $S_{st}$ | 3.969 | 3.967 | 3.967 |
| | $S_{panel}$ | 0.426 | 0.578 | 1.133 |
| | $S_c$ | 0.428 | 0.789 | 1.577 |
| n=10 (def.theory) | $S_{st}$ | 0.514 | 0.514 | 0.514 |
| | $S_{panel}$ | 0.405 | 0.437 | 0.470 |
| | $S_c$ | 0.405 | 0.451 | 0.493 |

such that it lies in the range $\sigma_{panel} < \sigma_c < \sigma_{st}$. We see here that an increase in the number of stiffeners can raise the values of $\sigma_{panel}$ considerably, and hence also the values of $\sigma_c$.

It is worthwhile at this stage to make a few remarks about the deformation theory results. In Figs. (3) the deformation theory values of $\sigma_{panel}$ and $\sigma_{st}$ are such that the flow theory values of $\sigma_c$ and that found using deformation theory differ by a relatively small amount. This may not always be the case, as some of the results in Table 1 show; in particular, for $N = 20$ and strain-hardening exponent $n = 10$, the two values of $\sigma_c$ differ significantly. So it appears that the large discrepancy between flow and deformation theory values of $\sigma_{st}$ (as in the case of cruciform column[12]) can affect the value of $\sigma_c$. A more detailed study is necessary, though, in order to determine how this discrepancy depends on material and geometrical properties.

In Figs. 4 we replotted the results shown in Figs. 3, this time showing how dimensionless critical load $P/Ert$ varies with stiffener size. As expected it is still possible for the total critical load to decrease despite an increase in overall cross sectional area.

(b) *Comparison of inside and outside stiffening*

The preceding set of results was repeated for shells with outside stiffening to examine the difference between externally and internally stiffened shells. Figures (5) show graphs of $\sigma_{out}/\sigma_{in}$ against $d/t$ for $d/t_s = 10$ and 5. In both cases, results are shown for elastic shells ($n = 1$) and for elastic-plastic shells having $\sigma_y/E = +0.002$ and $n = 3, 10$ (only flow theory was used here). The effects of having outside stiffeners is to cause an increase in critical stress. For $d/t_s = 2$, no graph is shown as $\sigma_{out}/\sigma_{in}$ was found to be $\sim 1.0$ for all cases. Also, for the plastic shells the effect of outside stiffeners is not as significant as for the elastic case, which one would of course expect since any potential increase in critical stress due to the shell having outside stiffeners is counteracted by the rapid decrease in material stiffeness in the plastic range. The results for the elastic case are very similar to those of Wang and Lin[4], who considered the relationship between critical stress and stiffener eccentricity, for stiffeners of constant cross sectional area. In the present case, though, the increase in eccentricity is associated with an increase in stiffener depth. It would appear that, the cases where $\sigma_{st} < \sigma_{panel}$ (Figs. 3(a), (b)) the decrease in value of critical stress with an increase in stiffener depth is to some extent offset by the increase when outside stiffeners are used. A note of caution is perhaps in order. In the case of heavily stiffened shells, the advantages gained by the use of outside stiffeners have to be

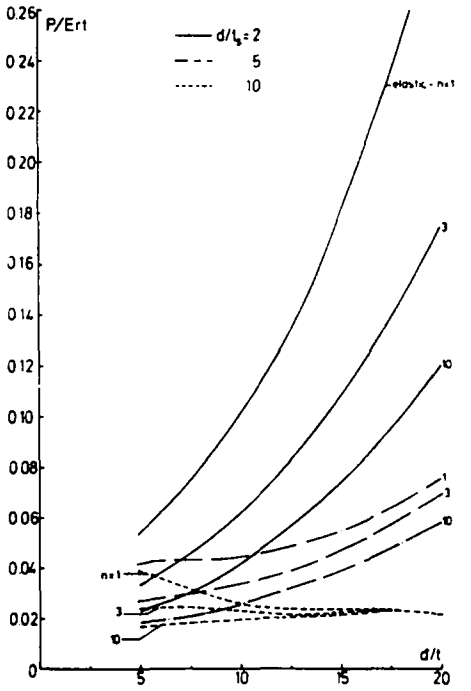


Fig. 4. Dimensionless critical total load $P/Ert$ vs $d/t_s$ for values of $d/t_s$ of 2, 5, 10, and for elastic and elastic-plastic materials. $\sigma_y/E = 0.002$ and elastic-plastic curves are for flow theory.

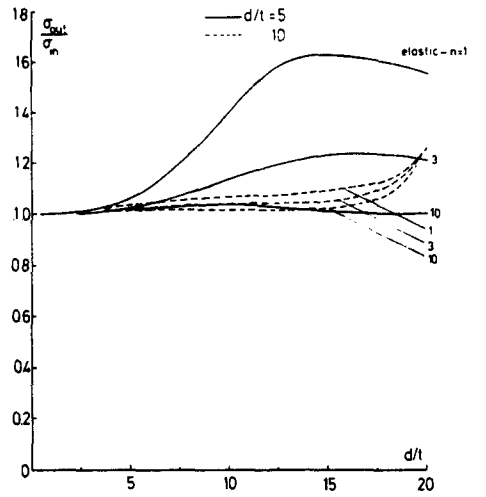


Fig. 5. Ratio of critical stress of externally stiffened shell to that of internally stiffened shell, vs $d/t$, for $d/t_s = 5$ and 10. $\sigma_y/E = 0.002$ and elastic–plastic curves are for flow theory.

considered in the light of an increase in imperfection-sensitivity[13]. The present analysis has not considered the effects of imperfection-sensitivity, but similar behaviour for sparsely-stiffened shells is a distinct possibility. In the plastic range, moreover, the rapid decrease in material stiffness would further contribute to the imperfection-sensitivity.

## 7. CONCLUDING REMARKS

The eigenvalue problem for buckling of a discretely stringer-stiffened cylindrical shell in axial compression has been formulated. The analysis given is an extension of that of Syngellakis and Walker[5] into the plastic range. Results are given for elastic shells, and for elastic–plastic shells using both $J_2$ flow and deformation theories.

Considerations of the effects of stiffener size on the critical stress have confirmed that, when the critical stress of a stiffener treated as a plate with one longitudinal edge free, is much lower than the critical stress of a simply-supported panel, the critical stress of the composite structure can fall significantly below that of the simply-supported panel. This observation contrasts with the suggestion[2, 7] that the critical stress of stiffened cylinders whose stiffeners have low torsional rigidity may be approximated by the simply-supported panel critical stress.

When the torsional rigidity of the stiffeners is high, through, the value of the $\sigma_{panel}$ is a lower bound to the critical stress of the composite shell, and it may be increased by increasing the number of stiffeners, i.e. by making the panels narrower. The limited study presented of the effects of increasing the number of stiffeners verifies this, and the value of $\sigma_c$ can be increased considerably by increasing the value of $\sigma_{panel}$.

Results for deformation theory indicate that the descrepancies between flow and deformation theory predictions of $\sigma_{st}$ and $\sigma_{panel}$ can in certain cases lead to a similar discrepancy for values of $\sigma_c$.

A comparison of critical stress of internally-stiffened shells with those of shells with outside stiffeners shows that where $\sigma_{st} < \sigma_{panel}$, the decrease in critical stresses with an increase in stiffener depth is to some extent offset by the increase when outside stiffeners are used. Although the effects of initial imperfections on the stiffened cylinders in the elastic range have been investigated[5, 6] consideration of these effects in the plastic range is still outstanding.

However, the analogy outlined between the behaviour of the stiffeners and that of an axially compressed cruciform column provides some important indicators. For it is well known that a cruciform column is extremely sensitive to initial imperfections in the plastic range[12]. Whether, and to what extent, this imperfection-sensitivity of the "cruciform-like" stiffeners affects that of the stiffened shell would seem to require further elucidation. In particular, whether any large discrepancy between flow and deformation theory values of $\sigma_{st}$ (and $\sigma_c$ for the stiffened shell) can be explained, as in the case of a cruciform column[12], in terms of the effects of initial imperfections, would be worth investigating.

*Acknowledgements*—The author is grateful to Dr. J. G. A. Croll for many helpful discussions during the preparation of this paper. This work was supported by the Science Research Council (U.K.).

## REFERENCES

1. J. Singer, M. Baruch and O. Harari, On the stability of eccentrically stiffened cylindrical shells under axial compression. *Int. J. Solids Structures* 3, 445–470 (1967).
2. W. T. Koiter, Buckling and post-buckling behaviour of a cylindrical panel under axial compression, NLR Rep. 5476. *Rep. Trans. Nat. Aero. Res. Inst.*, 20 (1956).
3. W. B. Stephens, Imperfection sensitivity of axially compressed stringer reinforced cylindrical panels under pressure. *AIAA J.* 9, 1713–1719 (1971).
4. J. T-S. Wang and Y-J. Lin, Stability of discretely stringer-stiffened cylindrical shells. *AIAA J.* 11, 810–814 (1973).
5. S. Syngellakis and A. C. Walker, Elastic buckling of stiffened cylindrical shells. *Int. Symp. on Integrity of Offshore Structures*, Glasgow (1978).
6. S. Syngellakis and A. C. Walker, Elastic local buckling of longitudinally stiffened cylinders. *Conf. on Stability Problems in Engng. Structures and Components*, Cardiff (1978).
7. V. Tvergaard, Buckling of elastic-plastic cylindrical panel under axial compression. *Int. J. Solids Structures.* 13, 957–970 (1977).
8. J. W. Hutchinson, Plastic buckling, *Advances in Applied Mechanics*, (Edited by C. S. Yih), Vol. 14, pp. 67–144. Academic Press, New York (1974).
9. B. Storåkers, On buckling of axisymmetric thin elastic-plastic shells, *Int. J. Solid Structures* 11, 1329–1346 (1975).
10. A. C. Walker and P. Davies, The collapse of stiffened cylinders. *Int. Conf. Steel Plated Structures*, Imperial College, London (1976).
11. S. Timoshenko and J. Gere, *Theory of Elastic Stability*, 2nd Edn. McGraw-Hill, Tokyo (1961).
12. J. W. Hutchinson and B. Budiansky, Analytical and numerical study of the effects of initial imperfections on the inelastic buckling of a cruciform column, Buckling of Structures, *Proc. IUTAM Symp.* (Edited by B. Budiansky), Cambridge, Massachusetts 1974, Springer (1976).
13. J. W. Hutchinson and J. C. Amazigo, Imperfection-sensitivity of eccentrically stiffened cylindrical shells. *AIAA J.* 5, 392–401 (1967).

## APPENDIX

The boundary conditions obtained from the line integrals, eqn (28), are given here. These are:

(a) for any panel, $x = 0, l$:

(i) $\hat{n}_x = 0$ or $\tilde{u} = 0$

(ii) $\hat{n}_{x\theta} = 0$ or $\tilde{v} = 0$

(iii) $\sigma_c t \tilde{w}_{,x} - \tilde{m}_{x,x} - (1/r)m_{x\theta,\theta} = 0$ or $\tilde{w} = 0$

(iv) $\tilde{m}_x = 0$ or $\tilde{w}_{,x} = 0$

(b) for the $i$th stiffener, i.e. at $\theta^{(i)} = \theta_0$:

(v) $$[\tilde{n}_{x\theta}]^{\theta^{(i)}+\eta\beta_0}_{\theta^{(i)}-\eta\beta_0} - \int_{-d}^{+d} (\tilde{N}_{x,x} + \tilde{N}_{xy,y})\,dy + [\tilde{N}_{xy}]^{y=d}_{y=-d} = 0 \quad \text{or} \quad \tilde{u} = 0$$

(vi) $$[\tilde{n}_\theta]^{\theta^{(i)}+\eta\beta_0}_{\theta^{(i)}-\eta\beta_0} + \int_{-d}^{d} (\tilde{M}_{x,xx} + 2\tilde{M}_{xy,xy} + \tilde{M}_{y,yy} - \sigma_c t_i \tilde{W}_{,xx})dy - [2\tilde{M}_{xy,x} + \tilde{M}_{y,y}]^{y=d}_{y=-d} = 0 \quad \text{or} \quad \tilde{v} = 0$$

(vii) $$[-(1/r)\tilde{m}_{\theta,\theta} - \tilde{m}_{x\theta,x}]^{\theta^{(i)}+\eta\beta_0}_{\theta^{(i)}-\eta\beta_0} - \int_{-d}^{d} (\tilde{N}_{xy,x} + \tilde{N}_{y,y})\,dy + [\tilde{N}_y]^{y=d}_{y=-d} = 0 \quad \text{or} \quad \tilde{w} = 0$$

(viii) $$[\tilde{m}_\theta]^{\theta^{(i)}+\eta\beta_0}_{\theta^{(i)}-\eta\beta_0} + \int_{-d}^{d} \{\sigma_c t_i \tilde{w}_{,xx} - (\tilde{M}_{x,xx} + 2\tilde{M}_{xy,xy} + \tilde{M}_{y,yy})\}(y-e)\,dy + \left[\tilde{M}_y + (2\tilde{M}_{xy,x} + \tilde{M}_{y,y})(y-e)\right]^{y=d}_{y=-d} = 0 \quad \text{or} \quad \tilde{w}_{,\theta} = 0$$

(ix) $$[\tilde{m}_{x\theta}]^{\theta^{(i)}+\eta\beta_0}_{\theta^{(i)}-\eta\beta_0} + \int_{-d}^{d} (\tilde{N}_{x,x} + \tilde{N}_{xy,y})(y-e)\,dy - [\tilde{N}_x(y-e)]^{y=d}_{y=-d} = 0 \quad \text{or} \quad \tilde{w}_{,x} = 0$$

(c) at $x = 0, l$, $y = \pm d$ and $\theta^{(i)} = \theta_0$:

(x) $\tilde{M}_{xy} = 0$ or $\tilde{v}, \tilde{w}_{,\theta} = 0$

(d) at $x = 0, l$ and $\theta^{(i)} = \pm\theta_0$:

(xi) $\tilde{m}_{x\theta} = 0$ or $\tilde{w} = 0$

(e) at $x = 0, l$ and $\theta^{(i)} = \theta_0$:

(xii) $\tilde{N}_x = 0$ or $\tilde{u}, \tilde{w}_{,x} = 0$

(xiii) $\tilde{N}_{xy} = 0$ $\tilde{w} = 0$

(xiv) $\sigma_c t_s \tilde{W}_{,x} - \tilde{M}_{x,x} - 2\tilde{M}_{xy,y} = 0$ or $\tilde{v}, \tilde{w}_{,\theta} = 0$

(xv) $\tilde{M}_x = 0$ or $\tilde{v}_{,x}\, \tilde{w}_{,\theta x} = 0$